TISSUE ENGINEERING: Part A
Volume 22, Numbers 11 and 12, 2016

DOI: 10.1089/ten.tea.2016.0103

termis
Tissue Engineering
& Regenerative Medicine
International Society

ORIGINAL ARTICLE

Three-Dimensional Environment Sustains Morphological Heterogeneity and Promotes Phenotypic Progression During Astrocyte Development

Swarnalatha Balasubramanian, PhD,[1] John A. Packard, BS,[1] Jennie B. Leach, PhD,[1] and Elizabeth M. Powell, PhD[2]

Astrocytes are critical for coordinating normal brain function by regulating brain metabolic homeostasis, synaptogenesis and neurotransmission, and blood–brain barrier permeability and maintenance. Dysregulation of normal astrocyte ontogeny contributes to neurodevelopmental and neurodegenerative disorders, epilepsies, and adverse responses to injury. To achieve these multiple essential roles, astrocyte phenotypes are regionally, morphologically, and functionally heterogeneous. Therefore, the best regenerative medicine strategies may require selective production of distinct astrocyte subpopulations at defined maturation levels. However, little is known about the mechanisms that direct astrocyte diversity or whether heterogeneity is represented in biomaterials. *In vitro* studies report lack of normal morphologies and overrepresentation of the glial scar type of reactive astrocyte morphology and expression of markers, questioning how well the *in vitro* astrocytes represent glia *in vivo* and whether *in vitro* tissue engineering methods are suitable for regenerative medicine applications. Our previous work with neurons suggests that the three-dimensional (3D) environment, when compared with standard two-dimensional (2D) substrate, yields cellular and molecular behaviors that more closely approximately normal ontogeny. To specifically study the effects of dimensionality, we used purified glial fibrillary acidic protein (GFAP)-expressing primary cerebral cortical astrocyte cultures from single pups and characterized the cellular maturation profiles in 2D and 3D milieu. We identified four morphological groups *in vitro*: round, bipolar, stellate, and putative perivascular. In the 3D hydrogel culture environment, postnatal astrocytes transitioned from a population of nearly all round cells and very few bipolar cells toward a population with significant fractions of round, stellate, and putative perivascular cells within a few days, following the *in vivo* ontogeny. In 2D, however, the population shift from round and bipolar to stellate and perivascular was rarely observed. The transition to distinct cellular morphologies in 3D corresponded to the *in vivo* expression of phenotypic markers, supporting the generation of mature heterogeneous glial populations *in vitro*. This study presents quantitative data supporting that 3D culture is critical for sustaining the heterogeneity of astrocytes *in vitro* and for generating a representation of the *in vivo* portfolio of heterogeneous populations of astrocytes required for therapeutic interventions in neurodevelopmental disorders, epilepsy, and brain injury.

Introduction

TRADITIONALLY, ADULT ASTROCYTES were considered as a homogeneous population that supports neuronal function.[1] In the last three decades, this view has changed to recognize that the *in vivo* astrocyte population is heterogeneous and dynamic, allowing the cells to perform a variety of complex functions in the central nervous system (CNS).[2–6] In the mouse, astrocytes are generated during the late embryonic and neonatal periods.[7–11] Astrocytes arise from neuroprogenitor cells after the generation of neurons,[12] and it is estimated that 10–15% of astrocytes derive from radial glia.[13] In the mouse, the first three postnatal weeks are a period of massive astrocyte expansion and migration, followed by maturation.[14]

During development, astrocytes guide the migration of neurons and direct axonal outgrowth and synapse formation.[15–19] Astrocyte dysfunction has been observed in developmental disorders of autism, Fragile X and Rett syndromes, as well as adult psychiatric diseases and seizure disorders.[20–26]

[1]Department of Chemical, Biochemical and Environmental Engineering, UMBC, Baltimore, Maryland.
[2]Departments of Anatomy and Neurobiology, Psychiatry, and Bioengineering, University of Maryland School of Medicine, Baltimore, Maryland.

In the healthy adult brain, astrocytes are responsible for functions, such as homeostasis of fluids, ions, pH, and neurotransmitters, as well as synaptic transmission and blood flow regulation.[5,27] Most recently, astrocytes have been reported to communicate with adjacent neurons using gliotransmitters and to have the capacity of neural stem cells (NSCs).[28] Upon injury, astrocytes have the potential to transform into a reactive state: become hypertrophied and release cytokines and extracellular matrix molecules to form a glial scar, which is hypothesized to prevent further tissue damage while severely impairing neuronal function.[29–32] Recent findings of reactive astrocytes in neurodegenerative disorders point to possible roles in Alzheimer's and Parkinson's diseases and amyotrophic lateral sclerosis.[25,33] It is not known if all astrocytes possess the capacity for the attributed functions or whether specific abilities are attributed to subpopulations of cells. Accumulating evidence supports astrocyte diversity with respect to developmental origin, morphology, gene expression, and function.

Astrocytes at different stages of postnatal development are morphologically and functionally diverse. At least four morphological forms of astroglial cells exist during astrocyte development: radial glial progenitors, proliferating intermediate progenitors, maturing postnatal astrocytes, and adult astrocytes, which include stellate and perivascular types.[34] Little is known about the mechanisms that regulate astrocyte heterogeneity or the pathways that favor astrocyte subtypes with therapeutic potential.[28] However, embryonic origin seems to contribute to astrocyte diversity, such that cerebral cortical astrocytes differ biochemically and physiologically from those generated by the hippocampus.[35] Numerous studies have highlighted differences in astrocyte gene expression in differential brain regions, with respect to injury response, and between *in vivo* and *in vitro* growth environments.[1,5,6,11,28,34,36] Thus, we propose that the development of more effective treatments requires a more detailed understanding of astrocyte heterogeneity and ontogeny in tissue engineering applications.

Currently, astrocytes are identified in mixed cultures from embryonic and neonatal brains by the expression of glial fibrillary acidic protein (GFAP). Often GFAP-expressing ($GFAP^+$) cells obtained from the differentiation of NSCs or induced pluripotent stem cells are surmised to be astrocytes. While astrocytes do express GFAP early in the postnatal period, adult astrocytes (especially gray matter protoplasmic astrocytes) exhibit little or no GFAP in the healthy CNS.[37] Rather, during normal ontogeny, GFAP expression is downregulated. Therefore, the current *in vitro* approaches do not generate phenotypic *in vivo* astrocytes, although newer isolation methods are narrowing the gap for short-term culture of adult astrocytes.[38] Thus, to achieve cells that represent the normal *in vivo* phenotypes and serve to redirect aberrant trajectories of human disease, better tissue engineering substrates and methods are required.

The standard method of isolating and culturing postnatal brain astrocytes in tissue culture polystyrene flasks was developed >30 years ago by McCarthy and de Vellis.[39] Although this method yields a high number of nearly pure GFAP immunoreactive astrocytes, recent work has established that astrocytes cultured on traditional two-dimensional (2D) substrates may not fully represent *in vivo* astrocytes. These astrocytes do not appear to progress through normal ontogeny through the downregulation of the early marker of GFAP and upregulation of mature astrocyte markers. The continued expression of GFAP has been interpreted to represent the reactive astrocyte phenotype,[40] yet these $GFAP^+$ astrocytes do not show hypertrophy of reactive astrocytes[41] or the glutamate-dependent calcium signaling of mature astrocytes.[42] We hypothesize that changing the culture environment can direct the purified astrocytes through normal ontogeny and provide a source for engineering astrocytes for clinical applications.

Three-dimensional (3D) cultures potentially provide a bridge between cell biological experiments, which employ 2D substrates (e.g., polystyrene, glass) and *in vivo* studies of cell behavior in the native 3D environment.[43,44] Our group has previously demonstrated that the morphology and signaling pathways of sensory neurons are dramatically altered when the cells are placed within a 3D versus 2D microenvironment, with the cellular response occurring in 3D collagen gels being a better representation of the *in vivo* scenario than 2D cultures.[45,46] In this work, we hypothesize that an engineered 3D microenvironment has the potential to direct astrocytes to follow innate programmed instructions to enable phenotypic diversity *in vitro*.

To characterize astrocyte heterogeneity with varying microenvironment dimensionality, we started with purified perinatal mouse cerebral cortical gray matter astrocytes and grew them on the traditional 2D collagen-coated coverslips and in 3D collagen gel in defined media. We observed distinctive differences in astrocyte morphology between 2D and 3D, specifically, a stellate-like morphology was observed in 3D, but not in 2D, cultures. We characterized physical and chemical conditions and their role in astrocyte phenotype determination. The work presented herein is a first step toward understanding astrocyte heterogeneity in 2D versus 3D culture. Our results indicate that astrocytes sense the dimensionality of their environment, and then modulate morphology, proliferation rate, and the expression of phenotypic markers. We report an improved *in vitro* culture method for producing astrocyte populations, which better reflects the *in vivo* cellular heterogeneity and allows observation of morphological and biochemical changes during normal maturation and in response to neuronal injury. Altogether, our quantitative findings suggest that the context of the cellular microenvironment is critical toward the progression of innate cellular programs.

Materials and Methods

Materials were obtained from Sigma-Aldrich or Invitrogen-Life Technologies unless otherwise noted.

Mice

$C57BL/6^J$ mice (Jackson Laboratory) were used. All animal studies were approved by the University of Maryland School of Medicine Institutional Animal Care and Use Committee and performed in accordance with NIH guidelines. The day of birth was counted as postnatal day (P) 1.

Astrocyte culture

Astrocytes were dissected from P1–P3 mouse cerebral cortices following standard protocols to isolate gray matter

astrocytes.[39] Astrocytes were expanded in tissue culture flasks (Corning) for 10–14 days and purified by shaking at 250 rpm for 8 h, after which the nonadherent cells were removed. This classic procedure yields cultures that were >98% astrocytes as assessed by positive GFAP immunoreactivity. Each flask contained the cells isolated from a single mouse pup cerebral cortex. Astrocytes were seeded at 7.5×10^3 cells/cm^2 onto 2D collagen-coated coverslips ($\sim$7 μg/cm^2) and at 7.5×10^5 cells/mL within 3D collagen gels (2 mg/mL, 25 μL) and then cultured for 4 or 10 days, with media changes every 2 days. The plating densities were chosen to reflect the densities of glial progenitors and astrocytes in the early postnatal brain.[47] In all cases, rat tail type I collagen (BD Biosciences) was used; methods to generate 2D coverslips and 3D gels were adapted from Ribeiro *et al.*[45]

Cells were maintained in serum-containing medium (Dulbecco's modified Eagle's medium [DMEM, high glucose, 4.5 g/L] supplemented with 10% fetal bovine serum and penicillin [100 U/mL] and streptomycin [100 μg/mL]) or in serum-free medium (DMEM supplemented with 1×N2 supplement and penicillin [100 U/mL] and streptomycin [100 μg/mL]). For 2 mg/mL collagen gels, ice-cold reagents, including 10×DMEM, 7.5% sodium bicarbonate, sterile deionized water, and collagen, were combined with cells to generate 3D substrates. The collagen/cell solution was allowed to gel in a culture incubator for 30 min before addition of culture medium. For each experiment, cells from a single flask were used for both 2D and 3D substrates. Unless otherwise noted, the cells were plated at 7.5×10^3 cells/cm^2 on 2D or 7.5×10^5 cells/mL in 3D. To test the effects of plating density, cells were plated at low (5×10^3 cells/cm^2 on 2D or 5×10^5 cells/mL in 3D), medium (7.5×10^3 cells/cm^2 on 2D or 7.5×10^5 cells/mL in 3D), and high density (1.5×10^4 cells/cm^2 on 2D or 1.5×10^6 cells/mL in 3D).

Immunofluorescence and image analysis

Samples were fixed in 24-well plates in buffered 4% formaldehyde solution for 20 min and permeabilized with Tris-buffered saline (TBS) containing 0.1% Triton X-100 and incubated with 10% lamb serum in TBS blocking solution for 30 min (in 2D) and 2 h (in 3D). The astrocytes were incubated in primary antibodies to GFAP (1:300; Abcam), S100β (1:300; Abcam), RC2 (1:250; Millipore), and nestin (1:300; Santa Cruz) for 1 h for 2D cultures, followed by appropriate fluorescently conjugated secondary antibodies (Jackson ImmunoResearch) for 30–60 min. A solution of 4′,6-diamidino-2-phenylindole (DAPI, 300 nM) was used to visualize cell nuclei. Immunofluorescence procedures for the 3D gels used the same antibody concentrations, but had longer washing steps (>30 min each) and overnight antibody incubations. Samples were imaged with confocal microscopy (Leica TCS SP5) and analyzed with LAS AF software (Leica) under the same confocal settings. For immunohistochemistry controls, some samples were incubated with only the primary or the secondary antibodies. Viability was assessed using the LIVE/DEAD assay according to the manufacturer's instructions (Molecular Probes Products, ThermoFisher Scientific).

Proliferation study

Cell proliferation during culture was measured using the Click-iT EdU kit (Life Technologies). Astrocytes were incubated with EdU for 4 days in culture, with media changes every 2 days. The cells were then fixed, permeabilized, incubated with Click-iT detection cocktail for 30 min for 2D cultures and overnight for 3D cultures, and followed by DAPI staining. Cell nuclei that proliferated during EdU incubation fluoresced green due to detection of EdU using AlexaFluor 488. DAPI (blue) stains all nuclei. The cultures were imaged and the numbers of EdU$^+$ and DAPI$^+$ cells were counted.

Statistical analyses

Each flask represented cells that were harvested from a single pup and therefore each flask represented an independent sample of cells ($\sim1\times10^6$). For each experiment, the cells from a single flask were tested in each of the dimensions: 2D and 3D (Fig. 1A). In some cases, the effects of medium composition (serum-containing or defined serum-free) were also tested. During each experiment, at least three to four individual cell populations (flasks) obtained from separate litters were evaluated. Plated cells were cultured for 4 or 10 days and then assessed for morphology, marker expression, and proliferation. For the characterization of cell morphology, 5–10 images were captured per sample, representing 50–100 cells for each sample. GFAP$^+$ cells were scored manually according to the morphologies defined in Figure 2A–F. Each experiment represents at least $n=3$ independent cell populations, and the experiments were repeated in triplicate. In Figure 3, the dataset passed the tests of normality and therefore statistically significant differences between experimental groups ($p<0.05$) as influenced by dimensionality and media were determined by two-way analysis of variance (ANOVA), followed by Holm–Sidak *post hoc* analyses, if appropriate. To determine the significance ($p<0.05$) of variation of cell group distribution due to the influence of culture parameters, we used a chi-square test. If the distributions were significantly different, then individual groups were compared using a Mann–Whitney rank sum test with a *t*-test for normally distributed data (determined by Shapiro–Wilk) or a Mann–Whitney U statistic.

Results

Effects of culture dimensionality on astrocyte morphology

To test whether 3D culture influences the morphological heterogeneity of astrocytes, we compared the morphology of astrocytes cultured at medium density: 7.5×10^3 cells/cm^2 on 2D collagen-coated coverslips and 7.5×10^5 cells/mL in 3D collagen gels (Fig. 1A). First, experiments were carried out for 4 days in serum-containing media, after which the cells were fixed and processed for GFAP immunoreactivity (Fig. 1B, C). Examination of the astrocyte morphologies revealed that distinct differences existed between cells cultured on 2D collagen-coated glass substrates and within 3D collagen gels (Fig. 2).

We identified three main groups of GFAP$^+$ astrocyte morphologies at 4-day culture period: round, bipolar, and stellate. Round astrocytes formed the majority of the population. On 2D substrates, round astrocytes were predominantly flat and large ($\sim$25 μm diameter) (Fig. 2A), while round astrocytes in 3D environment were relatively small ($\sim$10 μm) and spherical (Fig. 2B). Bipolar astrocytes had a small round soma with two opposing processes (Fig. 2C, D), resembling

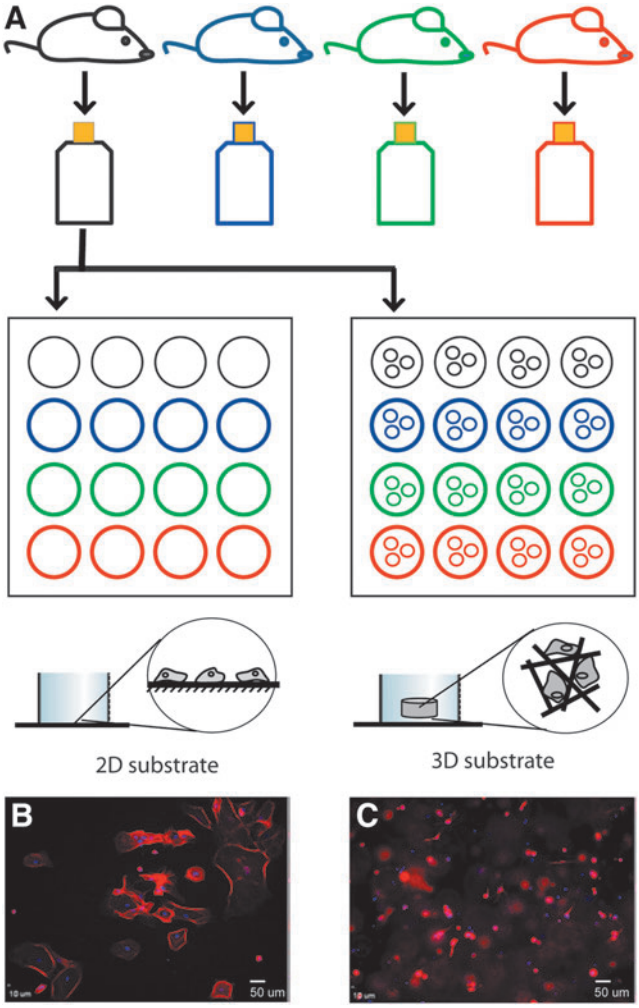

FIG. 1. Schematic of experimental strategy. **(A)** Gray matter cerebral cortical astrocytes were isolated from individual mouse pups at P1–P3. The astrocytes from a single pup are grown and purified in an individual flask and then used to compare the cellular responses to 2D and 3D environments. Each color represents an individual pup and cells obtained from it. Each experiment simultaneously compared astrocytes derived from three to four individual pups grown in 2D and 3D substrates and, in some cases, different medium formulations for each substrate. **(B)** Cells grown at a plating density of 7.5×10^3 cells/cm^2 on a 2D substrate appear as flattened cobblestones and are immunoreactive for GFAP (*red* fluorophore). **(C)** Cells grown within the 3D substrate (7.5×10^5 cells/ml) are distributed throughout the scaffold and are observed at multiple focal planes. The cells are immunoreactive for GFAP (*red* fluorophore) and appear much smaller than those in 2D **(B)**. DAPI (*blue*) is used to stain cell nuclei. Scale bar: 50 μm. 2D, two-dimensional; 3D, three-dimensional; GFAP, glial fibrillary acidic protein. Color images available online at www.liebertpub.com/tea

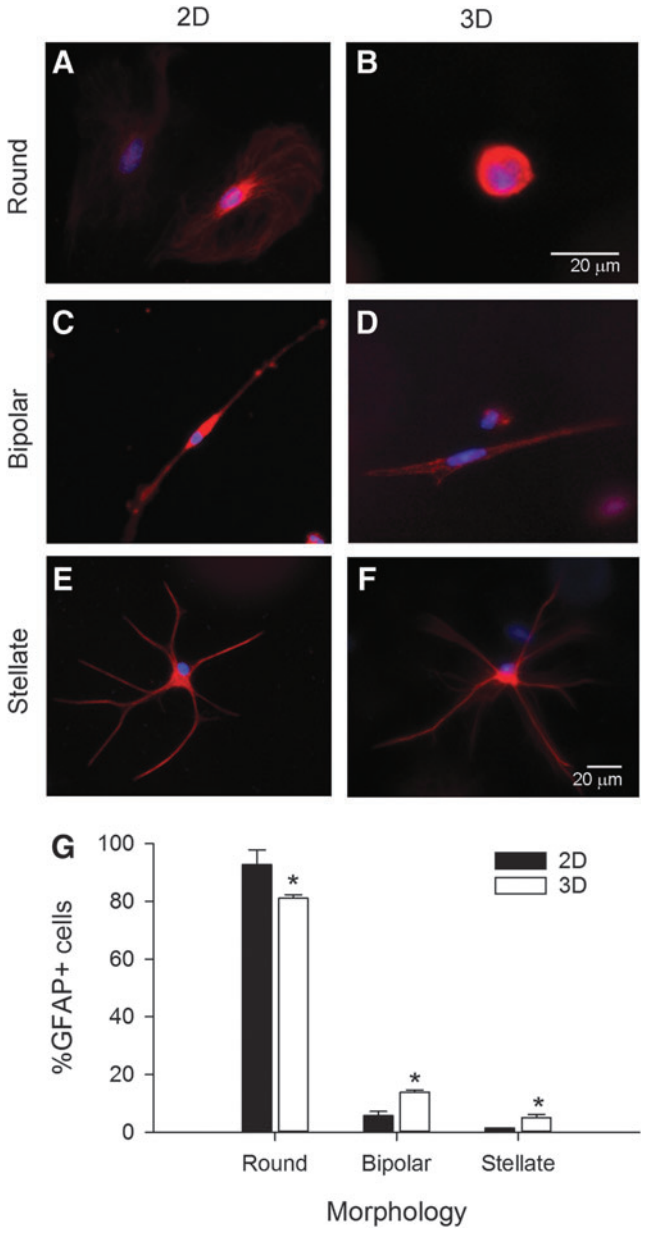

FIG. 2. Astrocytes exhibited unique profiles of morphologies dependent upon *in vitro* growth environment. Representative confocal images of primary astrocytes grown on 2D collagen-coated coverslips **(A, C, E)** or within 3D collagen gels **(B, D, F)** for 4 days in serum-containing media show immunoreactivity for the astrocyte marker, GFAP, as shown in *red* and cell nuclei are labeled with DAPI (*blue*). Multiple morphologies were observed in the GFAP$^+$ cells: round, without distinct processes or projections **(A, B)**, bipolar cells, which had two opposing processes **(C, D)**, and stellate cells, with multiple processes emerging from a centrally located soma **(E, F)**. The stellate cells resembled mature astrocytes *in vivo*. **(G)** Distribution of morphologies in 2D and 3D cultured substrates. *Asterisks* denote significant differences between the percentages of cells grown in 3D exhibiting each morphology compared with those on 2D substrates ($p < 0.001$ level). Scale bar: 20 μm. Please note that the cell in **(B)** is much smaller than the others. Color images available online at www.liebertpub.com/tea

the *in vivo* radial glial phenotype, and were observed both on 2D and in 3D cultures.[48–52] Stellate astrocytes resembled the star-shaped astrocytes found *in vivo* (Fig. 2E, F)[53–55] and were predominantly observed in 3D cultures. The unique morphologies of the GFAP$^+$ cells resemble the *in vivo* ontogeny from glial precursor to mature astrocyte. We observed significant differences in the distributions of morphologies of the

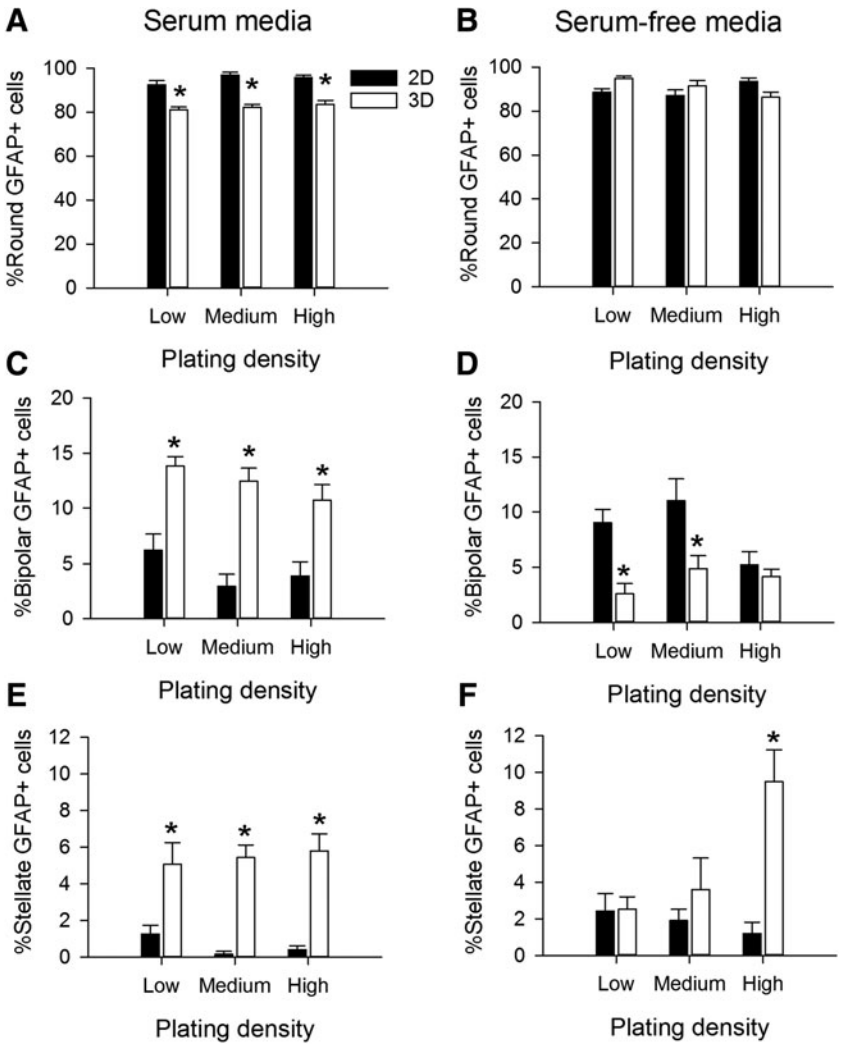

FIG. 3. Growth medium composition and substrate dimensionality contributed to the profiles of astrocyte morphologies. Astrocytes were cultured for 4 days in either serum-containing **(A, C, E)** or serum-free defined media **(B, D, F)**. Plating density was not a major factor determining the percentage of GFAP$^+$ cells with round **(A, B)**, bipolar **(C, D)**, or stellate morphologies **(E, F)**. Substrate dimension significantly altered each cell morphology category for all plating densities in serum media. Serum-free media induced significant distributions in cell morphologies that were dependent upon plating density and often different from serum-containing media. Dimensionality contributed dramatic shifts in the distributions of cell morphologies, with interactions with plating density and medium composition. For 2D experiments: low density is 5×10^3 cells/cm^2, medium density is 7.5×10^3 cells/cm^2, and high density is 1.5×10^4 cells/cm^2. For 3D experiments, low density is 5×10^5 cells/mL, medium density is 7.5×10^5 cells/mL, and high density is 1.5×10^6 cells/mL. Each bar represents the mean ± SEM of at least $n=3$ independent samples of >50 astrocytes per sample. An *asterisk* denotes a significant difference between cells comparing 2D and 3D substrates at the $p<0.05$ level.

GFAP$^+$ cells cultured on 2D and 3D substrates (Fig. 2G, $\chi^2=38.792$, $p<0.001$). In 3D, there were significantly fewer round cells ($t=9.047$, $p<0.001$), but more bipolar ($t=6.770$, $p<0.001$) and stellate cells ($t=45$, $p<0.001$). These data suggest that the substrate environment could influence glial ontogeny.

Quantitative assessment of astrocyte morphology in 2D and 3D environments

We initially tested the effects of several factors that may influence glial morphology and maturation after 4 days *in vitro*, including cell density, composition of the culture medium (serum-containing or serum-free), and dimensionality of the culture substrate (Supplementary Fig. S1 and Fig. 3; Supplementary Data are available online at www.liebertpub.com/tea). With serum-containing media, the majority of GFAP$^+$ cells on the 2D substrates plated at medium density were round (96% ± 1%) with a small number of cells appearing bipolar (4% ± 1%) or stellate (<1%). By comparison, in 3D at medium density, fewer of the GFAP$^+$ cells were round (83% ± 2%) and greater proportion of the cells were bipolar (13% ± 1%) or stellate (6% ± 1%). Comparing astrocytes grown in 2D, we observed overall differences in the distributions of morphologies with respect to serum content in the medium ($\chi^2=72.248$, $p<0.001$) and with respect to plating density in serum ($\chi^2=17.329$, $p=0.002$) and serum-free media ($\chi^2=18.463$, $p=0.001$, Supplementary Fig. S1A).

In 3D, the distributions of morphologies were different when comparing serum-containing and serum-free media ($\chi^2=88.211$, $p<0.001$ for low density, $\chi^2=57.769$, $p<0.001$ for medium density, and $\chi^2=56.884$, $p<0.001$ for high density, Supplementary Fig. S1B). However, the distributions of morphologies were not different when compared across densities in serum-containing medium ($\chi^2=2.468$, $p=0.650$). In the absence of serum, the distributions were different ($\chi^2=61.576$, $p<0.001$). Comparisons of the distributions with respect to dimensionality (2D vs. 3D) revealed that under all media and density conditions, astrocytes grown in 3D displayed different percentages of round, bipolar, and stellate cells than the same astrocyte population in 2D ($\chi^2>25.585$, $p<0.001$ for all comparisons).

The marked significant differences observed in the distributions of astrocyte morphologies led us to examine the effects of dimensionality, serum content, and density on the individual morphological groups. For clarity, data from each morphological group are presented in separate graphs (Fig. 3) to determine the effects of dimensionality and plating density. For round cells in serum-containing media, there was an effect of dimensionality ($F=163.168$, $p<0.001$), but no effect

of plating density ($F=1.847$, $p=0.169$, Fig. 3A). In serum-free media, the round phenotype was not affected by either dimensionality ($F=0.0474$, $p=0.828$) or plating density ($F=0.0784$, $p=0.925$, Fig. 3B). For the bipolar morphology, there was a main effect of dimensionality ($F=66.899$, $p<0.01$), but not plating density ($F=2.765$, $p=0.073$) in serum-containing media (Fig. 3C). In serum-free media, the bipolar shape was affected by both dimensionality ($F=17.893$, $p<0.001$) and plating density ($F=4.231$, $p=0.020$, Fig. 3D). Finally, for the stellate group of cells grown in serum-containing media, there was a main effect of dimensionality ($F=71.161$, $p<0.001$), but not plating density ($F=0.110$, $p=0.896$, Fig. 3E). In serum-free media, the stellate shape was affected by both dimensionality ($F=13.329$, $p<0.001$) and plating density ($F=3.430$, $p=0.041$), with a significant interaction between the parameters ($F=6.641$, $p=0.003$, Fig. 3F). Overall, dimensionality and serum content of the media had significant influences on all observed astrocyte morphologies. Because the impact of plating density was generally small and often not significant, we chose a standard density of 15,000 cells within 25 μL collagen gels (7.5×10^5 cells/mL) for the rest of the experiments.

Influence of physical location within the 3D environment on cell morphology

We independently tested the effects of the relative physical location in the gel to determine if the observed morphologies were the same throughout the substrate. Based on chi-square analysis, there was no effect of the physical position of the cells within the gel, that is, whether the cells were located in the center or near the edge in serum-containing ($\chi^2=9.511$, $p=0.484$, Supplementary Fig. S2A) or serum-free media ($\chi^2=3.301$, $p=0.192$, Supplementary Fig. S2B).

Effects of medium composition and culture dimensionality on astrocyte proliferation

We counted the total number of GFAP$^+$ cells after 4 days in culture and found an overall effect of dimensionality ($F=18.166$, $p<0.001$), but no effect of medium composition ($F=3.680$, $p=0.064$) and a significant dimension x serum interaction ($F=10.115$, $p=0.003$). *Post hoc* analysis revealed that significantly more cells were present after being grown in 3D with serum-free media ($p<0.001$, Fig. 4A). The total number of cells is the combined measure

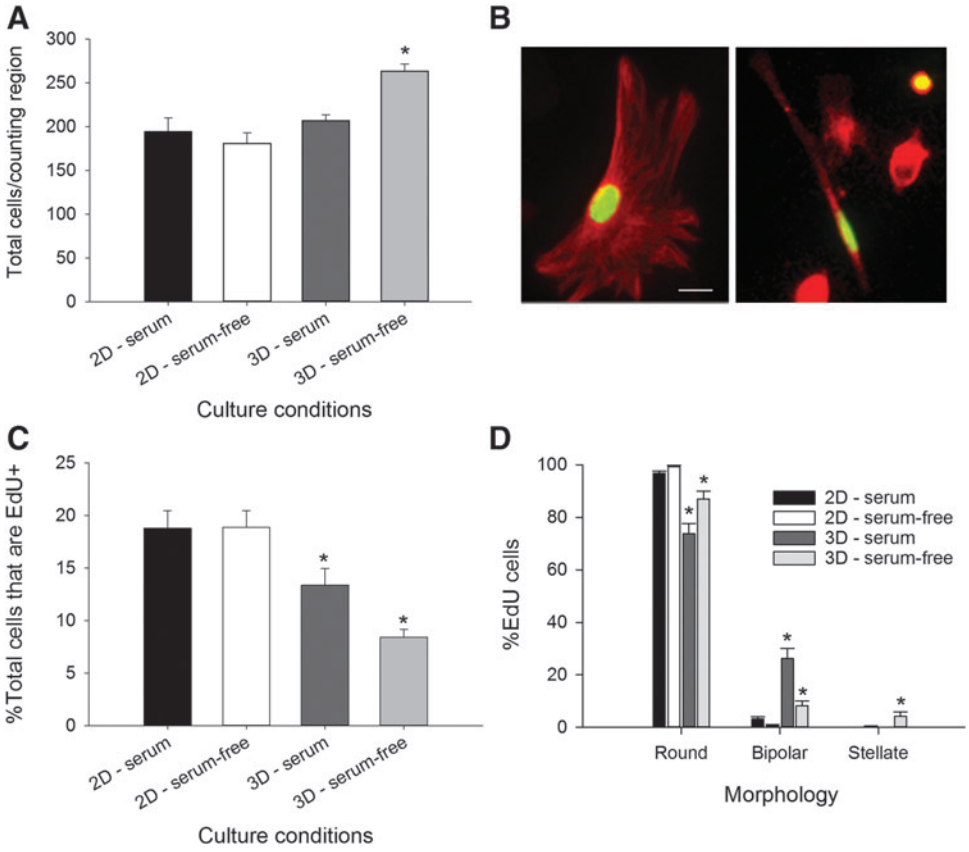

FIG. 4. Dimensionality and medium composition interact to alter cell proliferation and lineage. Astrocytes were cultured on 2D collagen-coated coverslips and within 3D collagen gels in serum-containing or serum-free media for 4 days. **(A)** The overall total number of cells, in equivalent regions, was increased in the 3D serum-free culture condition. **(B)** EdU was used to label cells that were in S-phase as a measure of cell proliferation. Double immunohistochemistry for GFAP (*red*) and EdU (*green*) demonstrates that round and bipolar astrocytes were among the proliferative populations. Bar = 10 μm. **(C)** Analysis of the percent of the population that had incorporated EdU yielded an effect of dimensionality. **(D)** The distribution of morphologies of EdU$^+$ cells was dependent upon medium composition and culture substrate dimension. Bars represent mean ± SEM from $n>3$ samples; in each sample, $n>50$ astrocytes were counted. An *asterisk* denotes a significant difference at the $p<0.05$ level for an effect of substrate dimension. Color images available online at www.liebertpub.com/tea

of the initial cells plated plus any born over 4 days minus those lost to cell death. To determine the influence of culture dimensionality and medium composition on astrocyte proliferation, we performed an EdU proliferation assay. EdU is a thymidine analog that is incorporated into DNA during the S-phase of cell division (Fig. 4B).[56] Analysis of the EdU incorporation provided an estimate of the newly born cells that exit the cell cycle. Cells that re-enter the cell cycle may lose the EdU signal through dilution of multiple divisions.[57–59] Our analysis revealed a main effect of dimension ($F=30.614$, $p<0.001$) and no effect of serum ($F=2.886$, $p=0.099$) or dimension×serum interaction ($F=57.878$, $p=0.087$). In serum-containing medium cultures, 19%±2% EdU^+ cells were observed in 2D compared with 13%±2% in 3D, and in serum-free media, 19%±2% EdU^+ were found in 2D compared with 8%±1% in 3D (Fig. 4C). In summary, dimensionality affected proliferation of $GFAP^+$ astrocytes and altered EdU^+ incorporation.

While counting the cells, we had the impression that more EdU^+ cells had bipolar and stellar morphologies. When we assessed the distributions of morphologies, they were significantly different with respect to dimensionality in serum-containing ($\chi^2=89.381$, $p<0.0001$) or serum-free cultures ($\chi^2=74.141$, $p<0.0001$) (Fig. 4D). Within each morphology, *post hoc* analysis revealed significant differences for the astrocytes grown in 3D, with main effects of dimension (round: $F=51.439$, $p<0.001$; bipolar: $F=50.348$, $p<0.001$; and stellate: $F=6.511$, $p=0.016$). In 3D, fewer cells adopted the round shape in serum-containing ($p<0.001$) and serum-free media ($p=0.001$). Similarly findings were found for bipolar cells (serum-containing, $p<0.001$ and serum-free, $p=0.017$). For the stellate shape, only cells grown in serum-free medium were significantly different ($p=0.001$). Overall, substrate dimensionality increased the proportion of proliferating astrocytes that exhibited the bipolar and stellate phenotypes.

Longer culture times reveal additional cell morphology

Astrocytes were cultured in parallel experiments in 3D gels for 4 and 10 days in serum and serum-free media. We examined cell viability using the LIVE/DEAD assay. Cell viability was estimated using the LIVE/DEAD assay. In 2D, 90%±9.5% viability was observed, whereas in 3D, 84%±8.6% were alive after 4 days ($t=2.66$, $p=0.004$). It should be noted that dead cells in the 2D condition are able to float away and thus are not counted, whereas in 3D, the cells are trapped and counted. Therefore, while the 2D cultures consistently had more viable cells, the size of the effect was modest.

After 10 days in culture, the distribution of morphologies was significantly different compared with 4 days ($\chi^2=423.387$, $p<0.001$), with decreased populations of round cells (73%±2% for serum and 75%±2% for serum-free) and bipolar cells (6%±1% for serum and 5%±0.5% for serum-free), but increased proportion of stellate cells (9%±1% for serum and 7%±1% for serum-free) (Fig. 5A).

An additional rare morphology that resembled a perivascular astrocyte was observed (11%±1% for serum and 12%±2% for serum-free). The putative perivascular-like astrocytes did not fit to the general morphology of the other three categories and had a long prominent process and multiple finer processes that appeared to be glial endfeet that contact blood vessels (Fig. 5B).[60] The perivascular-like cell was rarely present in the 4-day 3D cultures and was never observed in the 2D samples.

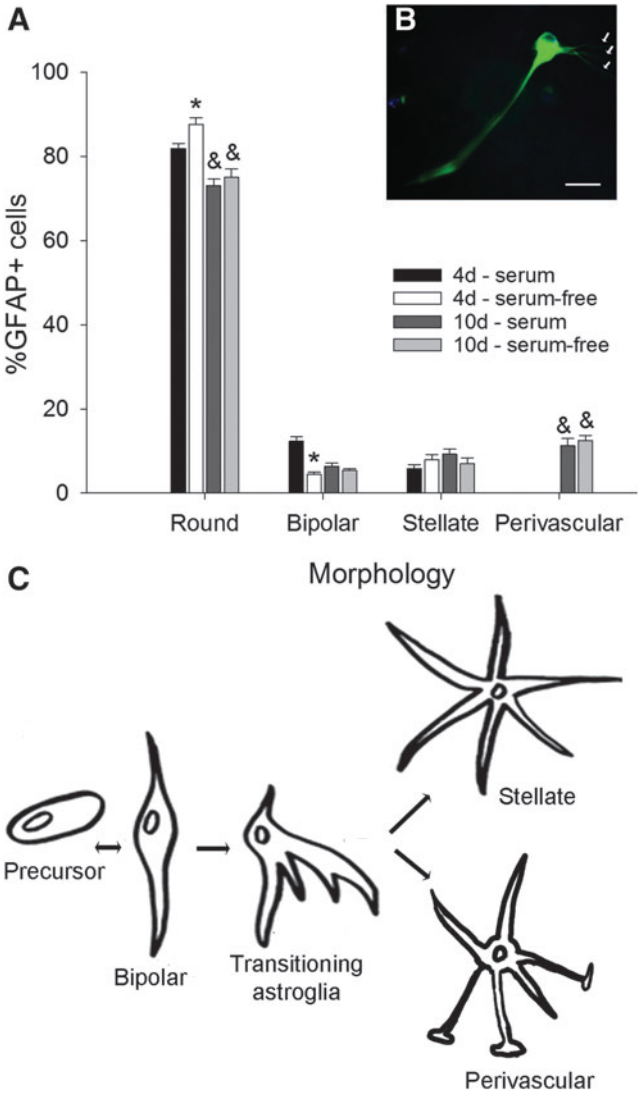

FIG. 5. Long-term culture in 3D substrates revealed a novel cell morphology. **(A)** Astrocytes were cultured in 3D substrates for 4 and 10 days in serum-containing and serum-free media. After 10 days in culture, fewer round astrocytes were observed, but the percent of bipolar and stellate cells remained similar to 4 days. However, a new type of cell that resembles the perivascular astrocyte proximal to blood vessels *in vivo* was observed. **(B)** The perivascular type of astrocyte is $GFAP^+$ and has a long central process and several fine endfeet. **(C)** Schematic of the progression of astrocyte phenotypes during perinatal maturation, adapted from Hunter and Hatten.[60] Bars represent mean±SEM from at least $n=3$ samples; in each sample, $n>50$ astrocytes were counted. *Asterisks* denote significant effect of medium composition ($p<0.05$), whereas *ampersands* show significant effects of time in culture ($p<0.05$). Scale bar: 20 μm. Color images available online at www.liebertpub.com/tea

Within each morphology, *post hoc* analysis revealed overall effects of time (round, $F=139.168$, $p<0.001$; bipolar, $F=9.016$, $p=0.005$; stellate, $F=10.361$, $p=0.003$; and perivascular, $F=317.11$, $p<0.001$, two-way ANOVA). Overall

effects of serum content in the media were observed for round ($F = 50.980$, $p < 0.001$) and bipolar cells, ($F = 58.651$, $p < 0.001$), but not stellate ($F = 2.251$, $p = 0.143$) and perivascular cells ($F = 3.309$, $p = 0.078$). In summary, time and serum content of the media affected the distribution of morphologies observed in the 3D substrates. A proposed model of astrocyte ontogeny is shown in Figure 5C, including the putative perivascular group.

Phenotypic characterization of astrocyte groups in 2D and 3D environments

Astrocytes express characteristic markers depending on the stage of development.[7,34,35,61–65] To correlate the astrocyte morphological populations with the *in vivo* phenotypes, we characterized astrocytes cultured on 2D collagen-coated coverslips and in 3D collagen gels for 10 days, with markers of cell development stage, including nestin,[66] RC2,[67] GFAP,[68] and S100β.[69,70] GFAP is an intermediate filament protein and a classic marker that is used in the immunocytochemical identification of astrocytes.[5] The RC2 antibody recognizes a 295 kDa intermediate filament proximal protein expressed in radial glial cells in the developing CNS.[67,71] S100β, a calcium-binding protein, is strongly expressed in mature astrocytes.[72–74] Nestin is an intermediate filament protein that is expressed in immature astroglial cells, but is absent in resting adult astrocytes.[75] Nestin is reexpressed in reactive astrocytes in response to injury or neurodegenerative disorders in the adult brain.[76,77] We investigated the expression of biochemical markers on the two largest morphological subgroups: round (Fig. 6) and bipolar cells (Fig. 7). Stellate and perivascular astrocytes were negligible on 2D cultures and present only in 3D cultures, and both populations expressed GFAP and S100β, but they did not show any immunoreactivity with RC2 or nestin. The stellate and perivascular cells were observed too infrequently to obtain quantitative expression data.

In 2D cultures, round astrocytes expressed GFAP and S100β in the same cells (99% ± 1%, Fig. 6A, B), with almost no coexpression of GFAP and RC2 (Fig. 6E, F) or GFAP and nestin. In 3D cultures, the coexpression of GFAP and S100β (Fig. 6C, D) was less, at 79% ± 3%, with 3% ± 1% of the $GFAP^+$ cells also expressing RC2 (Fig. 6G, H) and 12% ± 1% of the $GFAP^+$ cells coexpressing nestin. We analyzed the differences in biochemical marker expression (Fig. 6I) and found an overall effect of marker type ($F = 4535.912$, $p < 0.001$) and a significant dimension x marker interaction ($F = 82.573$, $p < 0.001$), but no overall effect of dimension ($F = 0.334$, $p = 0.566$). *Post hoc* analysis revealed that for S100β ($p < 0.001$) and nestin expression ($p < 0.001$), the percentages of $GFAP^+$ cells that coexpressed each marker in 3D were significantly different than 2D. No difference was observed for the RC2 marker ($p = 0.087$). Therefore, dimensionality of the substrate altered the S100β and nestin biochemical marker expression of the round astrocyte subpopulation.

Our initial observations of the bipolar astrocytes led us to propose that they may be radial glial cells, which express RC2 and nestin. Double immunocytochemistry for GFAP and S100β showed that while 85.1% ± 4.5% of the $GFAP^+$ astrocytes grown on 2D also express S100β, only 4.5% ± 1.2% of the $GFAP^+$ cells in 3D also expressed S100β (Fig. 7A–D). In contrast to the round cells, coexpression with RC2 (2D: 89.2% ± 3.0% and 3D: 96.2% ± 1.6%, Fig. 7E–H) and nestin (2D: 94.1% ± 3.0% and 3D: 94.5% ± 2.7%, Fig. 7I–M) was very high in the bipolar cells. Quantification of the percentages of the $GFAP^+$ astrocytes that expressed each marker shows the marked differences in S100β expression (Fig. 7N). We found main effects of dimension ($F = 109.349$, $p < 0.001$) and biochemical marker ($F = 193.847$, $p < 0.001$) and a dimension x marker interaction ($F = 145.761$, $p < 0.001$). Post hoc analysis revealed a significant difference between 2D and 3D substrates in S100β expression ($p < 0.001$), but not RC2 ($p = 0.087$) or nestin expression ($p = 0.931$). In summary, the bipolar cells on 2D coexpressed S100β, while those cultured in 3D expressed RC2 and nestin, markers found in radial glia.

Discussion

One of the major challenges in neural tissue engineering is defining the *in vivo* environment of the brain and the essential components for achieving the repair or regenerative environment.[2,28,78] For decades, neurons have been grown alone in/on biomaterials or devices, with some success, while the roles of astrocytes in normal development and disease and injury were being discovered. The current understanding of the astrocyte role in healthy neural function encompasses guidance of neurons and axons, synaptogenesis, formation of the blood–brain barrier, and inflammatory responses to injury and disease. Integrating the neuronal and astrocytic components for neural tissue engineering applications is stymied by our incomplete understanding of neurobiology and limited engineering tools and approaches.[79–82] Our approach has focused on a carefully defined astrocyte population and its response to several controlled parameters within the engineered environment. Our data suggest that perinatal cerebral cortical gray matter astrocytes are capable of progressing through normal ontogeny in an engineered 3D environment, providing a critical step to re-creating a receptive environment for normal neural function.[83,84]

In the brain, astrocytes are heterogeneous populations that differ in morphology, functional, and biochemical profiles, dependent upon their origin and developmental stage.[18,61] The most recent ideas suggest that astrocyte heterogeneity may direct brain regionality or NSC lineage.[85] Due to their heterogeneity, using astrocytes harvested from whole brains to evaluate biomaterials may obscure the different capacities of the substrates to support proliferation or specific functions. Therefore, we chose the well-studied perinatal cerebral cortical gray matter astrocytes.[16,39] While astrocytes have been successfully cultured, biochemical and morphological analyses indicate that cultured glia represent the reactive stages of ontogeny[40,61] and not the normal developmental trajectory.[18,34] Reactive astrocytes are commonly found *in vivo* after injury, in which the cells hypertrophy and release inflammatory cytokines and chemokines and generate extracellular matrix molecules that are hypothesized to inhibit nerve regeneration.[86–89]

Using standard techniques, astrocytes are often harvested, grown, and then expanded on 2D substrates.[39,90] Although 2D cultures have provided valuable biological insights, cells cultured in 3D culture may better represent the *in vivo* response in the healthy brain[91–95] because cells in 2D do not appear to achieve normal maturation. One of the fundamental differences of 2D versus 3D culture is the distribution of

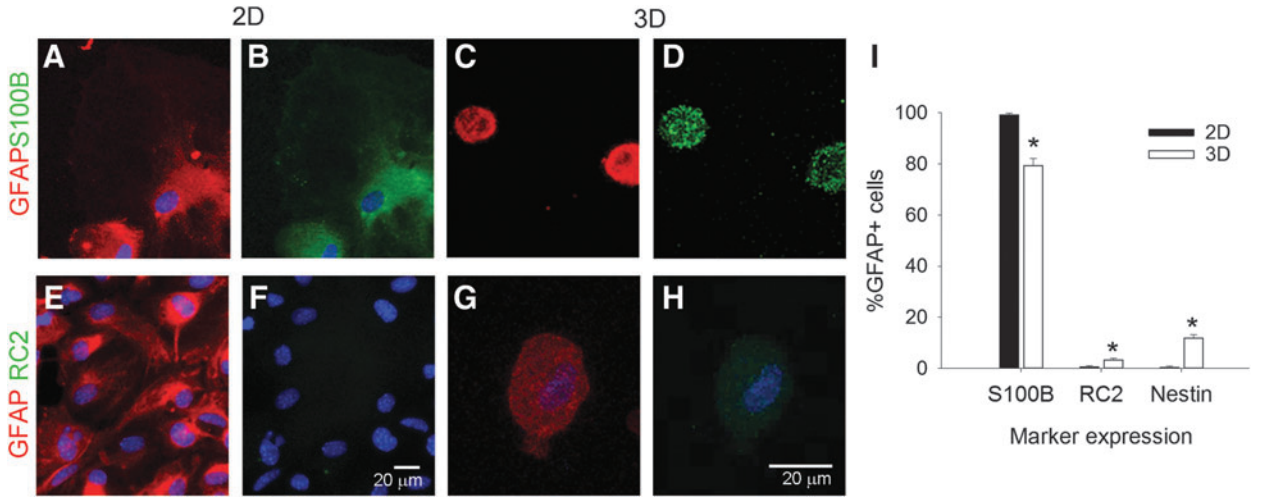

FIG. 6. Round GFAP$^+$ cells mainly express the astrocyte marker, S100β. Representative fluorescent images of round astrocytes cultured on 2D collagen-coated coverslips **(A, B, E, F)** and in 3D collagen gels **(C, D, G, H)**. Cells were colabeled for GFAP (*red*, **A, C, E, G)** and either S100β (**B, D**, *green*) or RC2 **(F, H)** or nestin. Cell nuclei were labeled with DAPI (*blue*). Scale bars: 20 μm. Please note the differences in cell size in 2D **(A, B, E, F)** and 3D **(C, D, G, H)**. **(I)** Analysis of immunoreactivity patterns shows that the majority of the round cells express S100β, with only a few that were grown in 3D-expressing RC2 or nestin. Bars represent mean ± SEM from at least $n = 3$ samples; in each sample, $n > 50$ astrocytes were counted. An *asterisk* denotes a significant difference at the $p < 0.05$ level. Color images available online at www.liebertpub.com/tea

cell–cell and cell–matrix interactions, which can alter signaling mechanisms regulating cell response.[96] We therefore hypothesized that a 3D culture may better maintain a heterogeneous astrocyte population characteristic of postnatal development in comparison with the 2D counterpart.

Astrocytes have been previously cultured in 3D electrospun scaffolds and in the Bioactive3D cell culture system, where astrocytes were treated as a single homogeneous population.[93,95] However, it is unclear whether these 3D culture systems support astrocyte heterogeneity and development *in vitro*. These reports used mixed cultures of gray and white matter astrocytes and did not follow the ontogeny and maturation processes. To characterize the populations of astrocytes that appear in 3D culture, we quantified astrocytes based on their morphology, marker expression, and proliferation to reflect reported differences in ontogeny. Focusing first on quantifying the heterogeneous astrocyte populations based on morphology (Fig. 2), we found that a 3D culture environment allows astrocytes to transition from a population of round and bipolar cells at 4 days toward a population with greater numbers of stellate and perivascular-like cells at 10 days. However, in 2D cultures, this population shift from round to bipolar involved a smaller fraction of the GFAP$^+$ population compared with 3D and yielded no stellate or perivascular cells (Fig. 5). Our results suggest that the dimensionality of the cellular microenvironment influences astrocyte ontogeny with 3D culture providing an aspect of the *in vivo* environment that allows early postnatal astrocytes to transition to the fully differentiated stellate morphology.

Next, we characterized astrocyte heterogeneity as influenced by various properties of the culture system, including the presence of serum, cell density, and location in the gel (edge vs. center). Previous reports have not investigated the effects of varying culture parameters on cell growth and maturation, including morphology and expression of biochemical markers. In comparison with 2D cultures, cells cultured in 3D may be more affected by restricted mass transfer of solutes throughout the gel and altered spatial distributions of cell and matrix ligands in the gel, thus leading to subpopulations dependent upon location. We observed that there is little influence on astrocyte heterogeneity with respect to location in the 3D substrates (Supplementary Fig. S2), likely due to the large pore size of collagen, which provides for a minimal barrier to solute transport.[97] These results suggest that macroporous gels such as collagen possess the architecture suitable to allow adequate solute transport.

The serum content of the media had the greatest effect on distribution of cell morphologies. We observed an interaction between dimensionality and serum content in the representation of bipolar and stellate groups (Fig. 3). These data imply that cell fate may be directed by a combination of serum-containing factors and microenvironment dimensionality and to a lesser extent cell density. Future studies will explore how the gels provide a 3D structure for ECM deposition and cell–matrix interactions that can drive cell maturation as these data are critical for scale-up to larger applications such as transplantation.

The different populations of astrocytes observed on 2D versus 3D culture could have resulted from differential rates of survival or proliferation between the morphological groups. We did observe a 6% difference in cell survival, with more dead cells being counted in 3D. This difference may be due to an underestimate of cell death in 2D as many cells lift from the substrate and are washed away in the media. A similar apparent increase in cell death was observed for rat astrocytes in 3D.[95] However, we do acknowledge that dead trapped cells may degrade over time, and the estimates of cell death in 3D may also be underestimated.

To address the issue of altered proliferation, we performed EdU incorporation assays (Fig. 4). Independent of dimensionality, round cells constituted the majority of proliferating cells, followed by bipolar cells, with negligible numbers of stellate cells dividing in culture. Yet, the 3D astrocyte cultures had fewer EdU$^+$ cells (8–13%), similar to that observed

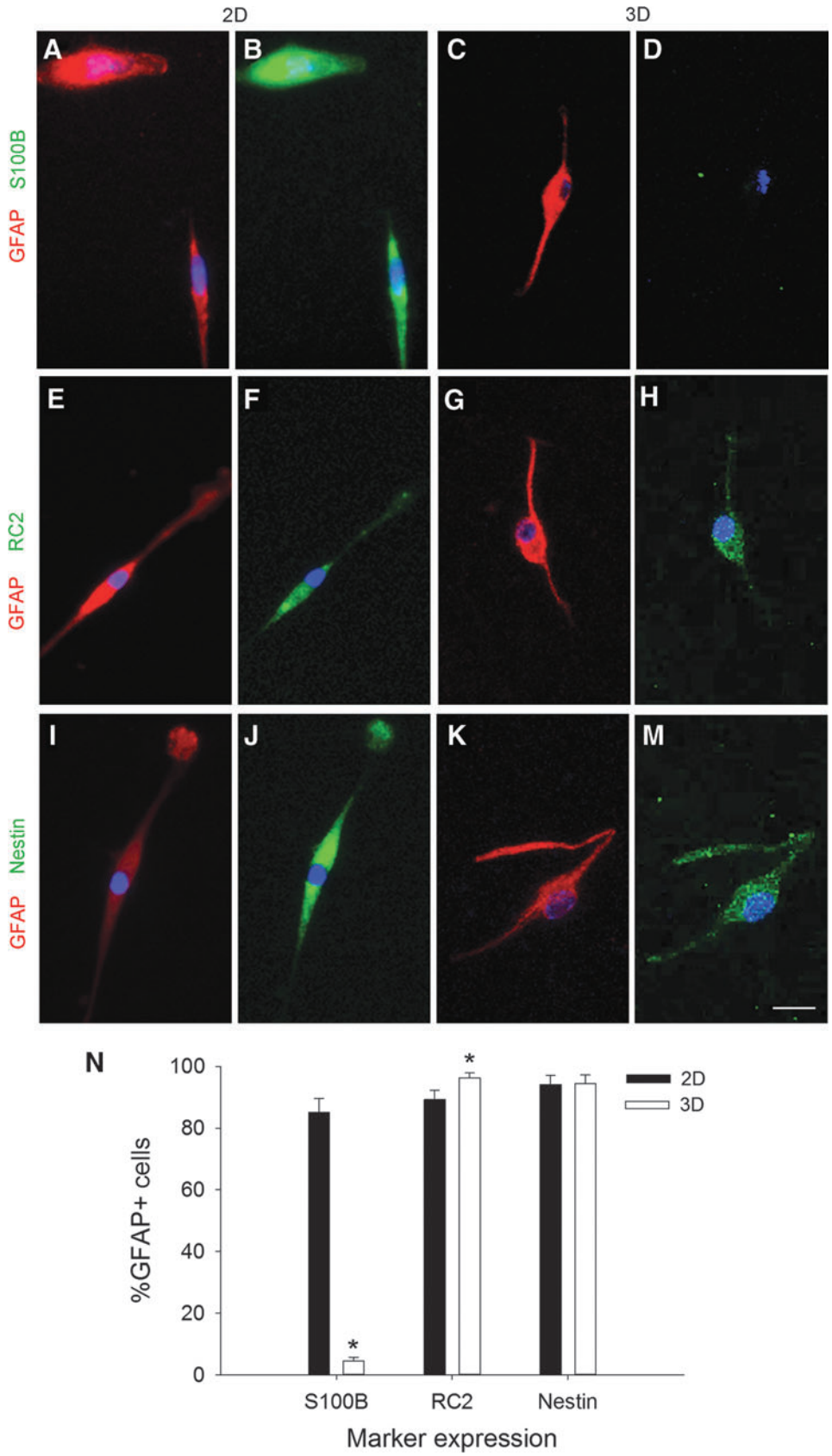

FIG. 7. Bipolar cells express phenotypic markers of radial glia. Representative images of bipolar cells cultured on 2D **(A, B, E, F, I, J)** or 3D substrates **(C, D, G, H, K, M)**. On 2D, the $GFAP^+$ (*red*) bipolar cells colabeled with the mature astrocyte marker, S100β **(B,** *green***)**, as well as the radial glial markers, RC2 **(F**, *green***)** and nestin **(J**, *green***)**. By contrast, in 3D, very few bipolar cells expressed S100β **(D)**, but nearly all expressed RC2 **(H)** and nestin **(M)**. Scale bar: 20 μm. **(N)** Expression of markers in bipolar cells. Bars represent mean ± SEM from at least $n = 3$ samples; in each sample, $n > 50$ astrocytes were counted. An *asterisk* denotes a significant difference at the $p < 0.05$ level. Color images available online at www.liebertpub.com/tea

in healthy cortex (9%).[2] On the contrary, 2D astrocyte cultures had more EdU^+ cells (19%) with higher proliferation similar to that observed in an injured cortex (20%) or suggesting an earlier maturation phase of the astrocytes that is observed during the first postnatal weeks.[98,99] Our proliferation results corroborate previous genomic studies that suggest that astrocytes isolated by the same methods[39] and cultured on 2D substrates are highly proliferative compared with healthy mature astrocytes and may represent reactive astroglial cells.[40] Furthermore, previous studies suggest that astrocytes proliferate faster in injured versus healthy adult brain,[100,101] and it is possible that the astrocytes sense the 3D environment as more akin to *in vivo* and proceed along a maturation pathway congruent with their biological age rather than continuing proliferation.

We note that while there was a marked increase in the populations of stellate and perivascular astrocytes in 3D culture, small round $GFAP^+$ cells are yet the predominate cell morphology. Previous literature from other cell types have also reported that cells cultured within 3D are smaller in apparent diameter than those cultured on 2D surfaces.[92,102] Furthermore, we speculate that the round phenotype of the majority of postnatal astrocytes in 3D is possibly because of lack of other essential growth factors that would otherwise allow them to transform into their mature form. This hypothesis is supported by the stable fraction of stellate astrocytes after 4 days of culture in 3D. Furthermore, *in vivo*, various growth factors, such as leukemia inhibitory factor and ciliary neurotrophic factor, are secreted by endothelial cells and early differentiated neurons and are known to promote astrocyte maturation.[11,22,103,104] Previous tissue engineering constructs have not evaluated the progression of glial maturation and therefore our study provides the first characterizations of the potential of 3D substrates to direct glial progenitors along specific cell lineages.

We then asked whether the morphological heterogeneity observed in culture corresponds to the *in vivo* astrocyte phenotypes that exist during development and in the adult. Recently human astrocytes were observed to have differential expression of GFAP and a range of shapes.[105] The relative expression of glial markers by astrocytes changes during development, varies between areas within the brain, and is influenced by cues in the extracellular environment.[7,34,61] Round astrocytes lacked a corresponding *in vivo*-like morphology, but expressed GFAP and S100β, which are markers for more mature astrocytic populations (Figs. 6 and 7). This result reinforces our hypothesis that additional factors may be required for the elaboration of a mature resting-state phenotype.

Radial glial cells are progenitors that can transform into neurons or astrocytes, depending on the stage of corticogenesis.[106,107] *In vivo*, astrocytes mature about 2 weeks after birth,[108] while radial glial cells that were present in the developing embryo disappear during this time.[109] In fact, after birth, the glial cells in the rodent brain expand six- to eightfold, with local sources, presumably radial glia, providing the initial glial pool.[110,111] During astrogliogenesis *in vivo*, radial glial cells progressively lose nestin and RC2 immunoreactivities and acquire a more ramified appearance and a stronger GFAP immunostaining.[112,113] Bipolar $GFAP^+$ cells present in 3D culture appear to be radial glial cells as characterized by morphology (Fig. 5C) and expression of both RC2 and nestin (Fig. 7).[51,71] We observed that in 3D culture, with an increase in culture time from 4 to 10 days, there was a reduction in the percentage of bipolar $RC2^+$ cells and an increase in stellate and perivascular astrocytes that do not express RC2 (Fig. 5B). Furthermore, the stellate and perivascular cells also do not express nestin, indicating that these $GFAP^+$ astrocytes have lost their progenitor potential and acquired a more mature developmental stage.[74,114] It is noteworthy that the bipolar astrocytes express S100β in 2D culture, but not in 3D culture. The molecule, S100β, is generally not expressed by radial glia *in vivo*.[112] Thus, the abnormal expression of S100β by radial glial cells could possibly be attributed to a stress response imposed by the artificial nature of 2D culture.[93]

In summary, we report that a 3D culture environment can sustain the morphology and heterogeneity of astrocytes observed *in vivo*. These findings suggest new ways of studying astrocyte development, behavior, and function *in vitro*. These studies also have significance in culturing populations of radial glial as well as mature nonreactive astrocytes in hydrogels for use in transplantation. Our ongoing work focuses on developing strategies to shift the astrocyte population toward specific phenotypes (e.g., radial glial progenitor cells) and defining the signaling mechanisms responsible for differences in astrocyte morphology observed in 2D versus 3D environments. By tailoring *in vitro* systems along specific trajectories, we can devise strategies to generate targeted cell populations from patient-derived progenitor or stem cells and also explore new mechanisms to altering *in vivo* milieu away from injury outcomes back to normal states and function.

Acknowledgments

The authors thank C. Petty for assistance with confocal microscopy and Dr. J. Loehe and Dr. C. Rakes for advice on statistical analysis. This work was supported by NIH-NINDS R01NS065205 (JBL and EMP) and a UMBC Undergraduate Research Award (JAP).

Disclosure Statement

The authors have no conflicts of interest to disclose.

References

1. Molofsky, A.V., and Deneen, B. Astrocyte development: a guide for the perplexed. Glia **63,** 1320, 2015.
2. Emsley, J.G., and Macklis, J.D. Astroglial heterogeneity closely reflects the neuronal-defined anatomy of the adult murine CNS. Neuron Glia Biol **2,** 175, 2006.
3. Kimelberg, H. Astrocyte heterogeneity or homogeneity? In: Parpura V., Haydon P.G., eds. Astrocytes in (Patho)physiology of the Nervous System. New York, NY: Springer, 2009, p. 1.
4. Matyash, V., and Kettenmann, H. Heterogeneity in astrocyte morphology and physiology. Brain Res Rev **63,** 2, 2010.
5. Sofroniew, M.V., and Vinters, H.V. Astrocytes: biology and pathology. Acta Neuropathol **119,** 7, 2010.
6. Oberheim, N.A., Goldman, S.A., and Nedergaard, M. Heterogeneity of astrocytic form and function. Methods Mol Biol **814,** 23, 2012.
7. Rusnakova, V., Honsa, P., Dzamba, D., Stahlberg, A., Kubista, M., and Anderova, M. Heterogeneity of astrocytes: from development to injury—single cell gene expression. PLoS One **8,** e69734, 2013.

8. Sturrock, R.R. Light microscopic identification of immature glial cells in semithin sections of the developing mouse corpus callosum. J Anat **122,** 521, 1976.
9. Raff, M.C., Fields, K.L., Hakomori, S.I., Mirsky, R., Pruss, R.M., and Winter, J. Cell-type-specific markers for distinguishing and studying neurons and the major classes of glial cells in culture. Brain Res **174,** 283, 1979.
10. Juurlink, B.H., Fedoroff, S., Hall, C., and Nathaniel, E.J. Astrocyte cell lineage. I. Astrocyte progenitor cells in mouse neopallium. J Comp Neurol **200,** 375, 1981.
11. Freeman, M.R. Specification and morphogenesis of astrocytes. Science **330,** 774, 2010.
12. Mione, M.C., Cavanagh, J.F., Harris, B., and Parnavelas, J.G. Cell fate specification and symmetrical/asymmetrical divisions in the developing cerebral cortex. J Neurosci **17,** 2018, 1997.
13. Rowitch, D.H., and Kriegstein, A.R. Developmental genetics of vertebrate glial-cell specification. Nature **468,** 214, 2010.
14. Bandeira, F., Lent, R., and Herculano-Houzel, S. Changing numbers of neuronal and non-neuronal cells underlie postnatal brain growth in the rat. Proc Natl Acad Sci U S A **106,** 14108, 2009.
15. Muller, C.M. Glial cell functions and activity-dependent plasticity of the mammalian visual cortex. Perspect Dev Neurobiol **1,** 169, 1993.
16. Powell, E.M., and Geller, H.M. Dissection of astrocyte-mediated cues in neuronal guidance and process extension. Glia **26,** 73, 1999.
17. Silver, J., Edwards, M.A., and Levitt, P. Immunocytochemical demonstration of early appearing astroglial structures that form boundaries and pathways along axon tracts in the fetal brain. J Comp Neurol **328,** 415, 1993.
18. Sloan, S.A., and Barres, B.A. Mechanisms of astrocyte development and their contributions to neurodevelopmental disorders. Curr Opin Neurobiol **27c,** 75, 2014.
19. Smith, G.M., Rutishauser, U., Silver, J., and Miller, R.H. Maturation of astrocytes *in vitro* alters the extent and molecular basis of neurite outgrowth. Dev Biol **138,** 377, 1990.
20. Yamamuro, K., Kimoto, S., Rosen, K.M., Kishimoto, T., and Makinodan, M. Potential primary roles of glial cells in the mechanisms of psychiatric disorders. Front Cell Neurosci **9,** 154, 2015.
21. Crawford, J.D., Chandley, M.J., Szebeni, K., Szebeni, A., Waters, B., and Ordway, G.A. Elevated GFAP protein in anterior cingulate cortical white matter in males with autism spectrum disorder. Autism Res **8,** 649, 2015.
22. Yang, Y., Higashimori, H., and Morel, L. Developmental maturation of astrocytes and pathogenesis of neurodevelopmental disorders. J Neurodev Disord **5,** 22, 2013.
23. Cao, F., Yin, A., Wen, G., Sheikh, A.M., Tauqeer, Z., Malik, M., Nagori, A., Schirripa, M., Schirripa, F., Merz, G., Brown, W.T., and Li, X. Alteration of astrocytes and Wnt/beta-catenin signaling in the frontal cortex of autistic subjects. J Neuroinflammation **9,** 223, 2012.
24. Bedner, P., Dupper, A., Huttmann, K., Muller, J., Herde, M.K., Dublin, P., Deshpande, T., Schramm, J., Haussler, U., Haas, C.A., Henneberger, C., Theis, M., and Steinhauser, C. Astrocyte uncoupling as a cause of human temporal lobe epilepsy. Brain **138,** 1208, 2015.
25. Verkhratsky, A., and Parpura, V. Neurological and psychiatric disorders as a neuroglial failure. Period Biol **116,** 115, 2014.
26. Edmonson, C., Ziats, M.N., and Rennert, O.M. Altered glial marker expression in autistic post-mortem prefrontal cortex and cerebellum. Mol Autism **5,** 3, 2014.
27. Perea, G., Navarrete, M., and Araque, A. Tripartite synapses: astrocytes process and control synaptic information. Trends Neurosci **32,** 421, 2009.
28. Zhang, Y., and Barres, B.A. Astrocyte heterogeneity: an underappreciated topic in neurobiology. Curr Opin Neurobiol **20,** 588, 2010.
29. Colangelo, A.M., Alberghina, L., and Papa, M. Astrogliosis as a therapeutic target for neurodegenerative diseases. Neurosci Lett **565,** 59, 2014.
30. Chen, Y., and Swanson, R.A. Astrocytes and brain injury. J Cereb Blood Flow Metab **23,** 137, 2003.
31. Smith, G.M., Miller, R.H., and Silver, J. Changing role of forebrain astrocytes during development, regenerative failure, and induced regeneration upon transplantation. J Comp Neurol **251,** 23, 1986.
32. Brodkey, J.A., Gates, M.A., Laywell, E.D., and Steindler, D.A. The complex nature of interactive neuroregeneration-related molecules. Exp Neurol **123,** 251, 1993.
33. Finsterwald, C., Magistretti, P.J., and Lengacher, S. Astrocytes: new targets for the treatment of neurodegenerative diseases. Curr Pharm Des **21,** 3570, 2015.
34. Molofsky, A.V., Krencik, R., Ullian, E.M., Tsai, H.H., Deneen, B., Richardson, W.D., Barres, B.A., and Rowitch, D.H. Astrocytes and disease: a neurodevelopmental perspective. Genes Dev **26,** 891, 2012.
35. Khakh, B.S., and Sofroniew, M.V. Diversity of astrocyte functions and phenotypes in neural circuits. Nat Neurosci **18,** 942, 2015.
36. Gotz, M., Sirko, S., Beckers, J., and Irmler, M. Reactive astrocytes as neural stem or progenitor cells: *in vivo* lineage, *In vitro* potential, and Genome-wide expression analysis. Glia **63,** 1452, 2015.
37. Kimelberg, H.K. The problem of astrocyte identity. Neurochem Int **45,** 191, 2004.
38. Foo, L.C., Allen, N.J., Bushong, E.A., Ventura, P.B., Chung, W.S., Zhou, L., Cahoy, J.D., Daneman, R., Zong, H., Ellisman, M.H., and Barres, B.A. Development of a method for the purification and culture of rodent astrocytes. Neuron **71,** 799, 2011.
39. McCarthy, K.D., and de Vellis, J. Preparation of separate astroglial and oligodendroglial cell cultures from rat cerebral tissue. J Cell Biol **85,** 890, 1980.
40. Zamanian, J.L., Xu, L., Foo, L.C., Nouri, N., Zhou, L., Giffard, R.G., and Barres, B.A. Genomic analysis of reactive astrogliosis. J Neurosci **32,** 6391, 2012.
41. Burda, J.E., and Sofroniew, M.V. Reactive gliosis and the multicellular response to CNS damage and disease. Neuron **81,** 229, 2014.
42. Sun, W., McConnell, E., Pare, J.F., Xu, Q., Chen, M., Peng, W., Lovatt, D., Han, X., Smith, Y., and Nedergaard, M. Glutamate-dependent neuroglial calcium signaling differs between young and adult brain. Science **339,** 197, 2013.
43. Baker, B.M., and Chen, C.S. Deconstructing the third dimension: how 3D culture microenvironments alter cellular cues. J Cell Sci **125,** 3015, 2012.
44. Tibbitt, M.W., and Anseth, K.S. Hydrogels as extracellular matrix mimics for 3D cell culture. Biotechnol Bioeng **103,** 655, 2009.
45. Ribeiro, A., Vargo, S., Powell, E.M., and Leach, J.B. Substrate three-dimensionality induces elemental morphological transformation of sensory neurons on a physiologic timescale. Tissue Eng Part A **18,** 93, 2012.
46. Ribeiro, A., Balasubramanian, S., Hughes, D., Vargo, S., Powell, E.M., and Leach, J.B. Beta1-integrin cytoskeletal

signaling regulates sensory neuron response to matrix dimensionality. Neuroscience **248c,** 67, 2013.
47. Savchenko, V.L., McKanna, J.A., Nikonenko, I.R., and Skibo, G.G. Microglia and astrocytes in the adult rat brain: comparative immunocytochemical analysis demonstrates the efficacy of lipocortin 1 immunoreactivity. Neuroscience **96,** 195, 2000.
48. Culican, S.M., Baumrind, N.L., Yamamoto, M., and Pearlman, A.L. Cortical radial glia: identification in tissue culture and evidence for their transformation to astrocytes. J Neurosci **10,** 684, 1990.
49. Dupouey, P., Benjelloun, S., and Gomes, D. Immunohistochemical demonstration of an organized cytoarchitecture of the radial glia in the CNS of the embryonic mouse. Dev Neurosci **7,** 81, 1985.
50. Pixley, S.K., and de Vellis, J. Transition between immature radial glia and mature astrocytes studied with a monoclonal antibody to vimentin. Brain Res **317,** 201, 1984.
51. Sild, M., and Ruthazer, E.S. Radial glia: progenitor, pathway, and partner. Neuroscientist **17,** 288, 2011.
52. Woodhams, P.L., Basco, E., Hajos, F., Csillag, A., and Balazs, R. Radial glia in the developing mouse cerebral cortex and hippocampus. Anat Embryol (Berl) **163,** 331, 1981.
53. Miller, R.H., and Raff, M.C. Fibrous and protoplasmic astrocytes are biochemically and developmentally distinct. J Neurosci **4,** 585, 1984.
54. Kalman, M., and Hajos, F. Distribution of glial fibrillary acidic protein (GFAP)-immunoreactive astrocytes in the rat brain. I. Forebrain. Exp Brain Res **78,** 147, 1989.
55. Bignami, A., and Dahl, D. Astrocyte-specific protein and radial glia in the cerebral cortex of newborn rat. Nature **252,** 55, 1974.
56. Krishan, A., and Hamelik, R.M. Click-iT proliferation assay with improved DNA histograms. Curr Protoc Cytom **7,** 7.36, 2010.
57. Glauche, I., Moore, K., Thielecke, L., Horn, K., Loeffler, M., and Roeder, I. Stem cell proliferation and quiescence—two sides of the same coin. PLoS Comput Biol **5,** e1000447, 2009.
58. Leydon, C., Bartlett, R.S., Roenneburg, D.A., and Thibeault, S.L. Localization of label-retaining cells in murine vocal fold epithelium. J Speech Lang Hear Res **54,** 1060, 2011.
59. Ganusov, V.V., and De Boer, R.J. A mechanistic model for bromodeoxyuridine dilution naturally explains labelling data of self-renewing T cell populations. J R Soc Interface 10, 20120617, 2013.
60. Hunter, K.E., and Hatten, M.E. Radial glial cell transformation to astrocytes is bidirectional: regulation by a diffusible factor in embryonic forebrain. Proc Natl Acad Sci U S A **92,** 2061, 1995.
61. Cahoy, J.D., Emery, B., Kaushal, A., Foo, L.C., Zamanian, J.L., Christopherson, K.S., Xing, Y., Lubischer, J.L., Krieg, P.A., Krupenko, S.A., Thompson, W.J., and Barres, B.A. A transcriptome database for astrocytes, neurons, and oligodendrocytes: a new resource for understanding brain development and function. J Neurosci **28,** 264, 2008.
62. Anthony, T.E., and Heintz, N. The folate metabolic enzyme ALDH1L1 is restricted to the midline of the early CNS, suggesting a role in human neural tube defects. J Comp Neurol **500,** 368, 2007.
63. Foo, L.C., and Dougherty, J.D. Aldh1L1 is expressed by postnatal neural stem cells *in vivo*. Glia **61,** 1533, 2013.
64. Hochstim, C., Deneen, B., Lukaszewicz, A., Zhou, Q., and Anderson, D.J. Identification of positionally distinct astrocyte subtypes whose identities are specified by a homeodomain code. Cell **133,** 510, 2008.
65. Appaix, F., Girod, S., Boisseau, S., Romer, J., Vial, J.C., Albrieux, M., Maurin, M., Depaulis, A., Guillemain, I., and van der Sanden, B. Specific *in vivo* staining of astrocytes in the whole brain after intravenous injection of sulforhodamine dyes. PLoS One **7,** e35169, 2012.
66. Lendahl, U., Zimmerman, L.B., and McKay, R.D. CNS stem cells express a new class of intermediate filament protein. Cell **60,** 585, 1990.
67. Misson, J.P., Edwards, M.A., Yamamoto, M., and Caviness, V.S., Jr. Identification of radial glial cells within the developing murine central nervous system: studies based upon a new immunohistochemical marker. Brain Res Dev Brain Res **44,** 95, 1988.
68. Bignami, A., and Stoolmiller, A.C. Astroglia-specific protein (GFA) in clonal cell lines derived from the G26 mouse glioma. Brain Res **163,** 353, 1979.
69. Olsson, J.E., Blomstrand, C., and Haglid, K.G. Cellular distribution of beta-trace protein in CNS and brain tumours. J Neurol Neurosurg Psychiatry **37,** 302, 1974.
70. Landry, C.F., Ivy, G.O., Dunn, R.J., Marks, A., and Brown, I.R. Expression of the gene encoding the beta-subunit of S-100 protein in the developing rat brain analyzed by *in situ* hybridization. Brain Res Mol Brain Res **6,** 251, 1989.
71. Pollard, S.M., and Conti, L. Investigating radial glia *in vitro*. Prog Neurobiol **83,** 53, 2007.
72. Brozzi, F., Arcuri, C., Giambanco, I., and Donato, R. S100B protein regulates astrocyte shape and migration via interaction with src kinase: implications for astrocyte development, activation, and tumor growth. J Biol Chem **284,** 8797, 2009.
73. Marshak, D.R. S100 beta as a neurotrophic factor. Prog Brain Res **86,** 169, 1990.
74. Steiner, J., Bernstein, H.G., Bielau, H., Berndt, A., Brisch, R., Mawrin, C., Keilhoff, G., and Bogerts, B. Evidence for a wide extra-astrocytic distribution of S100B in human brain. BMC Neurosci **8,** 2, 2007.
75. Eliasson, C., Sahlgren, C., Berthold, C., Stakeberg, J., Celis, J.E., Betsholtz, C., Eriksson, J.E., and Pekny, M. Intermediate filament protein partnership in astrocytes. J Biol Chem **274,** 23996, 1999.
76. Cho, J.M., Shin, Y., Park, J., Kim, J., and Lee, M. Characterization of nestin expression in astrocytes in the rat hippocampal CA1 region following transient forebrain ischemia. Anat Cell Bio **46,** 131, 2013.
77. Clarke, S.R., Shetty, A.K., Bradley, J.L., and Turner, D.A. Reactive astrocytes express the embryonic intermediate neurofilament nestin. Neuroreport **5,** 1885, 1994.
78. Garcia-Marques, J., and Lopez-Mascaraque, L. Clonal identity determines astrocyte cortical heterogeneity. Cereb Cortex **23,** 1463, 2013.
79. Aboody, K., Capela, A., Niazi, N., Stern, J.H., and Temple, S. Translating stem cell studies to the clinic for CNS repair: current state of the art and the need for a Rosetta stone. Neuron **70,** 597, 2011.
80. Lemmens, R., and Steinberg, G.K. Stem cell therapy for acute cerebral injury: what do we know and what will the future bring? Curr Opin Neurol **26,** 617, 2013.
81. Filbin, M.T. Recapitulate development to promote axonal regeneration: good or bad approach? Philos Trans R Soc Lond B Biol Sci **361,** 1565, 2006.
82. Emery, D.L., Royo, N.C., Fischer, I., Saatman, K.E., and McIntosh, T.K. Plasticity following injury to the adult central nervous system: is recapitulation of a developmental state worth promoting? J Neurotrauma **20,** 1271, 2003.

83. Harel, N.Y., and Strittmatter, S.M. Can regenerating axons recapitulate developmental guidance during recovery from spinal cord injury? Nat Rev Neurosci **7,** 603, 2006.
84. Gallo, V., and Deneen, B. Glial development: the crossroads of regeneration and repair in the CNS. Neuron **83,** 283, 2014.
85. Bayraktar, O.A., Fuentealba, L.C., Alvarez-Buylla, A., and Rowitch, D.H. Astrocyte development and heterogeneity. Cold Spring Harb Perspect Biol **7,** a020362, 2015.
86. Sofroniew, M.V. Molecular dissection of reactive astrogliosis and glial scar formation. Trends Neurosci **32,** 638, 2009.
87. Snow, D.M., Lemmon, V., Carrino, D.A., Caplan, A.I., and Silver, J. Sulfated proteoglycans in astroglial barriers inhibit neurite outgrowth *in vitro*. Exp Neurol **109,** 111, 1990.
88. Rudge, J.S., and Silver, J. Inhibition of neurite outgrowth on astroglial scars *in vitro*. J Neurosci **10,** 3594, 1990.
89. Smith, G.M., and Strunz, C. Growth factor and cytokine regulation of chondroitin sulfate proteoglycans by astrocytes. Glia **52,** 209, 2005.
90. Meiners, S., Powell, E.M., and Geller, H.M. A distinct subset of tenascin/CS-6-PG-rich astrocytes restricts neuronal growth *in vitro*. J Neurosci **15,** 8096, 1995.
91. Puschmann, T.B., de Pablo, Y., Zanden, C., Liu, J., and Pekny, M. A novel method for three-dimensional culture of central nervous system neurons. Tissue Eng Part C Methods **20,** 485, 2014.
92. Lai, Y., Cheng, K., and Kisaalita, W. Three dimensional neuronal cell cultures more accurately model voltage gated calcium channel functionality in freshly dissected nerve tissue. PLoS One **7,** e45074, 2012.
93. Puschmann, T.B., Zanden, C., De Pablo, Y., Kirchhoff, F., Pekna, M., Liu, J., and Pekny, M. Bioactive 3D cell culture system minimizes cellular stress and maintains the *in vivo*-like morphological complexity of astroglial cells. Glia **61,** 432, 2013.
94. Lau, C.L., Kovacevic, M., Tingleff, T.S., Forsythe, J.S., Cate, H.S., Merlo, D., Cederfur, C., Maclean, F.L., Parish, C.L., Horne, M.K., Nisbet, D.R., and Beart, P.M. 3D electrospun scaffolds promote a cytotrophic phenotype of cultured primary astrocytes. J Neurochem **130,** 215, 2014.
95. East, E., Golding, J.P., and Phillips, J.B. A versatile 3D culture model facilitates monitoring of astrocytes undergoing reactive gliosis. J Tissue Eng Regen Med **3,** 634, 2009.
96. Nelson, C.M., and Bissell, M.J. Of extracellular matrix, scaffolds, and signaling: tissue architecture regulates development, homeostasis, and cancer. Annu Rev Cell Dev Biol **22,** 287, 2006.
97. Wallace, D.G., and Rosenblatt, J. Collagen gel systems for sustained delivery and tissue engineering. Adv Drug Deliv Rev **55,** 1631, 2003.
98. Alonso, G. NG2 proteoglycan-expressing cells of the adult rat brain: possible involvement in the formation of glial scar astrocytes following stab wound. Glia **49,** 318, 2005.
99. Kornyei, Z., Czirok, A., Vicsek, T., and Madarasz, E. Proliferative and migratory responses of astrocytes to *in vitro* injury. J Neurosci Res **61,** 421, 2000.
100. Barreto, G.E., Sun, X., Xu, L., and Giffard, R.G. Astrocyte proliferation following stroke in the mouse depends on distance from the infarct. PLoS One **6,** e27881, 2011.
101. Myer, D.J., Gurkoff, G.G., Lee, S.M., Hovda, D.A., and Sofroniew, M.V. Essential protective roles of reactive astrocytes in traumatic brain injury. Brain **129,** 2761, 2006.
102. Grinnell, F. Fibroblast biology in three-dimensional collagen matrices. Trends Cell Biol **13,** 264, 2003.
103. Sakimoto, S., Kidoya, H., Naito, H., Kamei, M., Sakaguchi, H., Goda, N., Fukamizu, A., Nishida, K., and Takakura, N. A role for endothelial cells in promoting the maturation of astrocytes through the apelin/APJ system in mice. Development **139,** 1327, 2012.
104. Barnabe-Heider, F., Wasylnka, J.A., Fernandes, K.J.L., Porsche, C., Sendtner, M., Kaplan, D.R., and Miller, F.D. Evidence that embryonic the onset of cortical neurons regulate gliogenesis via cardiotrophin-1. Neuron **48,** 253, 2005.
105. Placone, A.L., McGuiggan, P.M., Bergles, D.E., Guerrero-Cazares, H., Quinones-Hinojosa, A., and Searson, P.C. Human astrocytes develop physiological morphology and remain quiescent in a novel 3D matrix. Biomaterials **42,** 134, 2015.
106. Voigt, T. Development of glial-cells in the cerebral wall of ferrets—direct tracing of their transformation from radial glia into astrocytes. J Comp Neurol **289,** 74, 1989.
107. Malatesta, P., Hartfuss, E., and Gotz, M. Isolation of radial glial cells by fluorescent-activated cell sorting reveals a neuronal lineage. Development **127,** 5253, 2000.
108. Kriegstein, A., and Alvarez-Buylla, A. The glial nature of embryonic and adult neural stem cells. Annu Rev Neurosci **32,** 149, 2009.
109. Wang, D.D., and Bordey, A. The astrocyte odyssey. Prog Neurobiol **86,** 342, 2008.
110. Ge, W.P., and Jia, J.M. Local production of astrocytes in the cerebral cortex. Neuroscience **323,** 3, 2016.
111. Ge, W.P., Miyawaki, A., Gage, F.H., Jan, Y.N., and Jan, L.Y. Local generation of glia is a major astrocyte source in postnatal cortex. Nature **484,** 376, 2012.
112. Raponi, E., Agenes, F., Delphin, C., Assard, N., Baudier, J., Legraverend, C., and Deloulme, J.C. S100B expression defines a state in which GFAP-expressing cells lose their neural stem cell potential and acquire a more mature developmental stage. Glia **55,** 165, 2007.
113. Burns, K.A., Murphy, B., Danzer, S.C., and Kuan, C.Y. Developmental and post-injury cortical gliogenesis: a genetic fate-mapping study with Nestin-CreER mice. Glia **57,** 1115, 2009.
114. Eng, L.F. Glial fibrillary acidic protein (GFAP): the major protein of glial intermediate filaments in differentiated astrocytes. J Neuroimmunol **8,** 203, 1985.

Address correspondence to:
Elizabeth M. Powell, PhD
Departments of Anatomy & Neurobiology, Psychiatry, and Bioengineering
University of Maryland School of Medicine
HSF II S251, 20 Penn Street
Baltimore, MD 21201

E-mail: epowel@gmail.com

Jennie B. Leach, PhD
Department of Chemical, Biochemical & Environmental Engineering
UMBC
Eng 314, 1000 Hilltop Circle
Baltimore, MD 21250

E-mail: jleach@umbc.edu

Received: March 16, 2016
Accepted: May 17, 2016
Online Publication Date: June 1, 2016